Renal tuberculosis mimicking xanthogranulomatous pyelonephritis: ultrasonography, computed tomography and magnetic resonance imaging findings

İzlem İzbudak-Öznur[1], Sinan Sözen[2], Sedat Işık[1]

Departments of [1]Radiology, and [2]Urology, Gazi University Faculty of Medicine, Ankara, Turkey

SUMMARY: İzbudak-Öznur İ, Sözen S, Işık S. Renal tuberculosis mimicking xanthogranulomatous pyelonephritis: ultrasonography, computed tomography and magnetic resonance imaging findings. Turk J Pediatr 2002; 44: 168-171.

The incidence of tuberculosis has been increasing in recent years, and its treatment has also become challenging. The diagnosis of renal tuberculosis is often difficult and delayed. Early and correct diagnosis of tuberculosis with different organ system involvement is very important and can be easier with ultrasonography, computed tomography and/or magnetic resonance imaging. Although renal tuberculosis is the result of hematogenous spread more commonly from the lungs, less than 5%, of patients with urinary tract tuberculosis have active pulmonary disease.

Renal tuberculosis may show variable radiological findings depending on the stage of the infection. Although an end-stage "autonephrectomized" kidey in tuberculosis is classically defined to be small in size, enlargement may on rare occasions be observed, which is the case in our patient. This form greatly mimics diffuse xanthogronulomatous pyelonephritis. Both diseases show thickening of the perirenal fasciae and spread of inflammation into the adjacent organs. Computed tomography and magnetic resonance imaging may show some specific features to differentiate these two entities.

Key words: kidney, tuberculosis, xanthogranulomatous pyelonephritis; ultrasound; computed tomography; magnetic resonance imaging.

Renal tuberculosis (TB) is almost always the result of hematogenous spread from the respiratory system, and occasionally from bones or the gastrointestinal tract. A spectrum o findings may be present depending on the stage of infection and the degree of host response. Advanced renal TB with fibrosis and stricture in the renal pelvis and total calyceal hydronephrotic/pyonephrotic appearance with renal calculi may mimic diffuse xanthogranulomatous pyelonephritis (XGP).

Case Report

A 16-year-old female patient, who was otherwise healthy, presented with intermittent left flank pain and a history of recurrent urinary tract infections. A tender mass in the left upper quadrant was palpated. Laboratory data revealed anemia (hemoglobin: 8.4 g/dl), leukocytosis (WBC count: $17x10^3/mm^3$), and urine culture positive for Proteus species and normal blood urea nitrogen, serum creatinine and liver function tests.

Scout kidney-ureter-bladder (KUB) film revealed multiple calculi and an irregular group of calcifications overlying the lower pole of the left kidney. Intravenous pyelogram (IVP) showed a nonfunctioning left kidney (Fig. 1). Ultrasonography (USG) revealed a large reniform shaped mass in the left renal bed with multiple variably echo-poor areas, probably corresponding to dilated calyces. Calculi and calcifications with distal shadowing were observed (Fig. 2). Anothner large heterogeneous mass posterior to the kidney extending into the left psoas muscle was identified. On computed tomography (CT), an enlarged kidney with a preserved reniform outline and marked peripelvic fibrosis was demonstrated. No calculus or calcification was observed in the renal pelvis but they were present in the lower pole calyces and parenchyma (Fig. 3).

Multiple low-density ovoid areas, consistent with a hydronephrotic pattern with a surrounding rim of tissue, that strongly enhanced with intravenous contrast media, were observed. Perirenal and lateroconal fasciae were markedly thickened. The ureter and renal vascular pedicle could not be identified. CT demonstrated a huge left psoas abscess also involving the quadratus lumborum muscle. Dystrophic calcifications were observed within the abscess (Fig. 4). On CT scans the tail of the pancreas and spleen were displaced anteriorly and superiorly by the enlarged left kidney, and fat planes in between were obliterated. Lumbar vertebrae were normal. Magnetic resonance imaging (MRI) revealed an enlarged left kidney with prominent calyceal dilatation and cortical thinning. Corticomedullary differentiation was lost. On T2-weighted (TR/TE/NEX=2560/90/2) axial images, negative defects within some calyces corresponding to calculi were observed. Perirenal fasciae were thickened and showed a low signal on T2-weighted images, indicating fibrotic changes or thick fibrinous exudates. A mass lesion overlying the left psoas and quadratus lumborum muscles was observed. The contours of the pancreas anterior to the kidney were edematous, but the interface between the kidney and spleen was preserved. Postcontrast TI-weighted (660/21/1.5) images showed marked contrast enhancement of thinned cortex, thickened perirenal fasciae and psoas mass (Fig. 5).

Transabdominal nephrectomy was performed. The renal mass was yellowish in color, extremely firm and immobile. An abscess extending into the psoas and quadratus lumborum muscles was drained. Microscopic evaluation revealed giant granulomas with central caseification necrosis, peripheral giant cells, fibroblasts and lymphocytes consistent with tuberculosis.

Fig. 1. Intravenous pyelogram shows nonfunctioning left kidney with multiple calculi and punctate calcifications overlying the lower pole (→).

Fig. 2. Transverse sonogram of the left kidney shows diffuse renal enlargement with irregular contour and multiple hypoechoic areas probably corresponding to dilated calyces (→). Parenchyma-sinus differentiation is lost. Small calculi and calcifications with distal shadowing are observed (→).

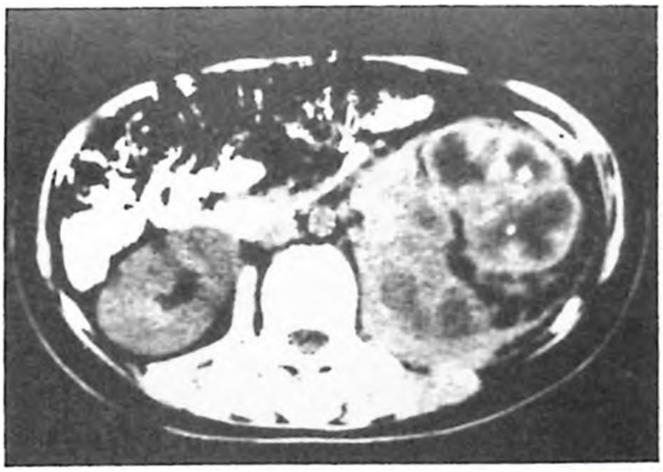

Fig. 3. CT reveals an enlarged left kidney with a preserved reniform outline and a hydronephrotic pattern (→). Small calculi and punctate calcifications are observed (→). Marked peripelvic, periureteric fibrosis; an abscess extending into the left psoas and quadratus lumborum muscles and thickened perirenal fasciae are demonstrated (→).

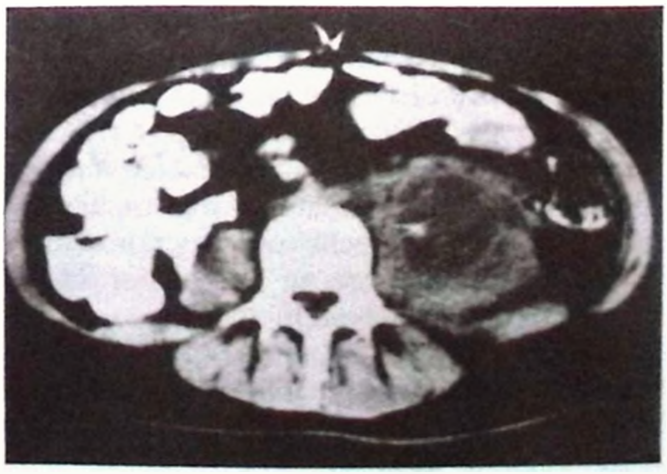

Fig. 4. CT shows calcification within the psoas abscess (→).

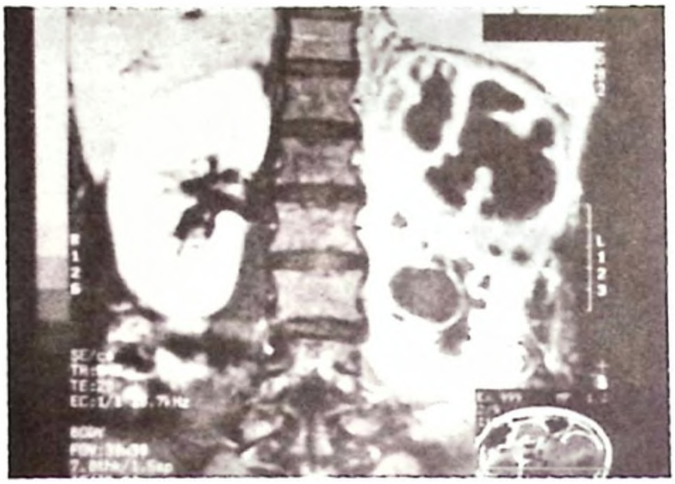

Fig. 5. Coronal postcontrast TI-weighted (660121/1.5) MR image demonstrates an upwardly and laterally displaced hydronephrotic left kidney with marked cortical thinning (→). Corticomedullary differentiation is lost. A hugee psoas abscess with hypointense necrotic foci and showing marked contrast enhancement is observed (→). Perirenal fasciae are thickened, but spleen, lumbar vertebrae and lateral abdominal wall are not involved.

Discussion

The diagnosis of renal TB is often difficult and delayed. Although renal TB is the result of hematogenous spread more commonly from the lungs, less than 5% of patients with urinary tract TB have active pulmonary disease. Radiographic evidence of past pulmonary TB is observed in less than 50% of patients[1]. No evidence of present or past pulmonary TB was observed in our patient. The median age of such patients is 50 years, and renal involvement is rare before the age of 20.

Early renal TB is usually bilateral, asymptomatic and stable. In more advanced disease, however, studies have shown that the macroscopic morphologic renal abnormalities visible on imaging modalities are almost always unilateral. The reasons for asymmetry of the gross findings in a disease in which early stages are symmetric remain unclear. Advanced disease is a result of focal disease progressing into tuberculous abscess (tuberculoma) that may rupture into the collecting system. A schirrous reaction will be stimulated and stenosis or obstruction of the involved collecting system will occur, which results in focal renal TB. If the disease process extends to involve the renal pelvis, total calyceal hydronephrosis will occur. The progressive granulomatous destruction of the kidney with fibrosis and subsequent obstructive uropathy will produce an "autonephrectomy" that is end-stage renal TB. At this stage, the nonvisualized kidney at urography which may be small, normal or enlarged in size is best evaluated with sonography or CT, which may show a hydronephrotic/pyonephrotic or solid granuloma pattern. Cortical thinning is observed overlying the affected calyces partly because of the resultant ischemia and partly due to an obstructive pyonephrosis[2]. Dystrophic parenchymal calcifications often develop. Involvement of the pararenal spaces with the spread of inflammation is an expected finding.

Xanthogranulomatous pyelonephritis is an uncommon chronic renal inflammation in which renal parenchyma are destroyed and replaced by lipid-laden macrophages. It is usually seen in middle-aged women, but pediatric cases have also been reported[3,4]. Unilateral diffuse involvement with urolithiasis is observed in 70-80% of then cases. Usually there is an enlarged nonfunctioning hydronephrotic kidney with pelvic calculi. Patients complain of recurrent urinary tract infections. Proteus mirabilis and Escherichia coli are the most commonly implicated organisms. Extrarenal extension to peri- and pararenal spaces is common. The process may involve more remote sites such as psoas muscles, subphrenic and pleural spaces, spleen, colon, abdominal wall and skin[5,6]. Anemia and leukocytosis were noted in most of the patients[7].

Our case, a 16-year-old female with left flank pain, showed anemia, leukocytosis and urine culture positive for Proteus mirabilis. IVP revealed multiple calculi and calcifications within a unilateral nonfunctioning kidney. USG, CT and MRI examinations demonstrated a diffusely enlarged kidney with contracted and fibrotic renal pelvis and multicystic cavities arranged in a hydronephrotic pattern. Perirenal extension and involvement of the ipsilateral psoas and quadratus lumborum muscles were also noted. Cortical thinning showing contrast enhancement was observed on both CT and MR scans. However, contrast material was not excreted into the hydronephrotic spaces. The psoas abscess also showed marked contrast enhancement. CT revealed nephrolithiasis and multiple small calcifications within the renal parenchyma. Punctate calcifications were also noted in the psoas abscess.

This case illustrates many radiologic and clinical characteristics suggestive of XGP. However, although calculous XGP may occur in up to 20%

of cases, complete or incomplete staghorn calculus within the renal pelvis is the most characteristic finding of XGP, and this was not present in our patient. In renal TB, dystrophic parenchymal calcifications often develop as a complication of renal papillary necrosis. Such calcific foci may detach from the papilla, or a completely necrotic papilla may slough into the pyelocalyceal system which then calcifies, resulting in calculus formation or putty-like calcification. Nevertheless, this process usually does not lead to the formation of staghorn calculi. Moreover, calcifications within an extrarenal inflammatory mass lesion is not noted in XGP, but it may be an expected finding in TB. In our patient, CT successfully demonstrated punctate calcifications within the psoas abscess. We suggest this finding may be helpful to consider a correct diagnosis of TB. Additionally, Goldman et al.[2] reported that in chronic inflammatory process of the kidney with periureteric or peripelvic fibrosis, TB must be considered. There was marked peripelvic and periureteric fibrosis in our patient, and the ureter could not be identified separately. Pelvic fibrosis may be observed in XGP but it usually accompanies the pelvic staghorn calculus.

Although an end-stage "Autonephrectomized" kidney in TB is classically defined to be small in size, enlargement on rare occasions may be observed, and this should be considered in the differential diagnosis. CT and MRI are very useful tools in addition to the IVP and USG and provide specific information aiding the correct diagnosis.

REFERENCES

1. Becker JA. Renal tuberculosis. Urol Radiol 1988; 10: 25-30.
2. Goldman SM,Fishman EK, Hartman DS, Kim YC, Siegelman SS. Computed tomography of renal tuberculosis and its pathological correlates. J Comput Assist Tomogr 1985; 9: 771-776.
3. Kural AR, Akaydın A, Öner A, et al. xanthogranulomatous pyelonephritis in children and aluts. Br J Urol 1987; 59: 383-385.
4. Hammadeh MY, Nicholls CJ, Buick RG, Gomall P, Corkery JJ. Xanthogranulomatous pyelonephritis in childhood: preoperative diagnosis is possible. Br J Urol 1994; 73: 83-86.
5. Eastham J, Ahledng T, Skinner E. Xanthogranulomatous pyelonephritis: clinical findings and surgical considerations. Urology 1994; 43: 295-299.
6. Goldman SM, Hartman DS, Fishman EK, Finizio JP, Gatewood OM, Siegelman SS. CT of xanthogranulomatous pyelonephritis. radiologic-pathologic correlation. AJR 1984; 141: 963-969.
7. chuang CK, Lai MK, Chang PL, et al. Xanthogranulomatous pyelonephritis experience 36 cases. J Urol 1992; 147: 333-336.